University of Sistan and Baluchestan

Challenges in Nano and Micro Scale Science and Technology

Online ISSN: 2821 - 000X

Treatment of Lung Cancer Using Magnetic Nanoparticles Hyperthermia: Simulation Based Study and Cardiac Thermal Safety

Kazhal Moetamedi[1] | Mohammad Hossein Tavakoli[2] | Zahra Keshtpour Amlashi[3] | Safoora Nikzad[4]

1. Department of Physics, Faculty of Sciences, Bu-Ali Sina University, Hamedan, Iran
2. Corresponding Author, Department of Physics, Faculty of Sciences, Bu-Ali Sina University, Hamedan, Iran. Email: mht@basu.ac.ir
3. Cancer Research Center, Institute of Cancer, Avicenna Health Research Institute, Hamadan University of Medical Sciences, Hamadan, Iran
4. Department of Medical Physics, Faculty of Medicine, Hamadan University of Medical Sciences, Hamadan, Iran

Article Info

Article type:
Research Article

Keywords:
Finite Element Simulation,
Lung Cancer,
Magnetic Hyperthermia,
Magnetic Nanoparticles,
Respiratory Dynamics,
Thermal Modeling

ABSTRACT

Magnetic hyperthermia is an emerging, minimally invasive modality for targeted cancer therapy, utilizing magnetic nanoparticles (MNPs) to induce localized heating within tumors. This study presents a comprehensive simulation-based analysis of magnetic hyperthermia applied to lung cancer. A two-dimensional axisymmetric finite element model was developed, incorporating key anatomical components tumor, air cavity, muscle, bone, skin to evaluate spatial thermal profiles under physiological respiratory dynamics. Magnetite (Fe_3O_4) nanoparticles (19 nm) were subjected to an alternating magnetic field (AMF) at 300 kHz and current intensity 300 A to induce localized heating through Néel and Brownian relaxation mechanisms. The model assessed thermal propagation during inhalation and exhalation, targeting tumor ablation temperatures (42–46 °C). Simulation results confirm the feasibility and thermal safety of MNP-assisted magnetic hyperthermia for lung cancer. These findings offer a clinically relevant framework for optimizing treatment planning and nanoparticle design. The novelty of this study lies in the development of a physiologically accurate finite element simulation that incorporates respiratory dynamics. This integrated approach, combining porous media modeling with thermal distribution analysis under dynamic breathing phases, offers new insights into optimizing safe and effective hyperthermia treatments for thoracic malignancies.

INTRODUCTION

Magnetic hyperthermia therapy (MHT) has emerged as a promising, minimally invasive strategy for cancer treatment, leveraging the ability of magnetic nanoparticles (MNPs) to convert electromagnetic energy into localized heat when subjected to an alternating magnetic field (AMF). By elevating tumor temperatures to the therapeutic range (42–46 °C), MHT promotes apoptosis, enhances tumor perfusion, and potentiates the efficacy of chemotherapy and radiotherapy, while minimizing damage to surrounding healthy tissues.

While MHT has demonstrated promising results in preclinical and clinical studies targeting glioblastoma, breast, and prostate cancers [1–3], its application to lung cancer remains underexplored due to the thoracic cavity's complex anatomy and the proximity of critical structures such as the bronchi, and vasculature. These anatomical constraints pose significant challenges in achieving effective and localized thermal delivery without inducing off target heating or. To address these challenges, computational modeling has gained traction as a predictive and optimization tool for hyperthermia planning. Multiphysics simulations enable the integration of magnetic field dynamics, nanoparticle thermogenesis, blood perfusion, and tissue-specific heat transfer, thus offering insights into thermal dose distribution under realistic physiological conditions [4–6].

In this study, we present a finite element-based, two-dimensional axisymmetric model that simulates magnetic hyperthermia for lung tumors, incorporating detailed

How to Cite this paper: Moetamedi K. Tavakoli M.H. Keshtpour Amlashi Z. Nikzad S. Treatment of Lung Cancer Using Magnetic Nanoparticles Hyperthermia: Simulation Based Study and Cardiac Thermal Safety. *Challenges in Nano and Micro Scale Science and Technology*. 2024; 12(1): 58-65. DOI: 10.22111/cnmst.2025.52359.1264

DOI: 10.22111/cnmst.2025.52359.1264

anatomical structures, respiratory airflow dynamics, and cardiac proximity. We use magnetite (Fe_3O_4) nanoparticles, which are widely accepted for clinical hyperthermia due to their biocompatibility. The simulations assess thermal distribution during respiratory cycles (inhalation and exhalation) under standard AMF exposure conditions. By simulating a physiologically accurate lung environment, this work provides a robust computational foundation for optimizing treatment parameters and ensuring safe, effective hyperthermia delivery for thoracic oncology applications. Our results are contextualized against recent experimental studies and propose directions for translational research in nanoparticle-assisted lung cancer therapy.

MATERIALS AND METHODS

Problem Definition

A two-dimensional axisymmetric model of tumor geometry within human lung tissue was developed to simulate magnetic hyperthermia treatment. Figure 2 depicts the anatomical structure of the lung, with an approximated tissue height of 13 cm. The tumor, representing lung cancer, was modeled as a circular region with a diameter of 1 cm, located adjacent to porous lung tissue and the airway. This configuration reflects the typical anatomical arrangement, ensuring clinical relevance and accuracy [8–11].

The Finite Element Method (FEM) was employed to solve the governing heat transfer equations and model the complex interactions between the alternating magnetic field and biological tissues. FEM is a powerful numerical technique that enables precise modeling of complex geometries and the solution of partial differential equations describing physical phenomena such as heat conduction and electromagnetic interactions. By discretizing the domain into finite elements, the method facilitates detailed analysis of thermal and magnetic effects within heterogeneous tissue structures [12–19].

For simplicity and uniformity, the distribution of magnetic nanoparticles (MNPs) within the tumor tissue was assumed homogeneous. Magnetite (Fe_3O_4) nanoparticles were selected due to their excellent biocompatibility, magnetic responsiveness, and chemical stability [20–25].

Heat generation within the tumor tissue arises predominantly from Néel and Brownian relaxation mechanisms. These phenomena enable magnetic nanoparticles to convert electromagnetic energy into thermal energy through internal magnetic moment relaxation and physical rotational motion, respectively. The generated heat elevates tumor temperature to therapeutic levels (42–46 °C), inducing apoptosis in cancer cells while minimizing thermal damage to adjacent healthy tissues [25–29]. Figure 1 Schematic representation of the tumor geometry within human lung tissue, highlighting the circular shape of the tumor and its location adjacent to muscle tissue and air.

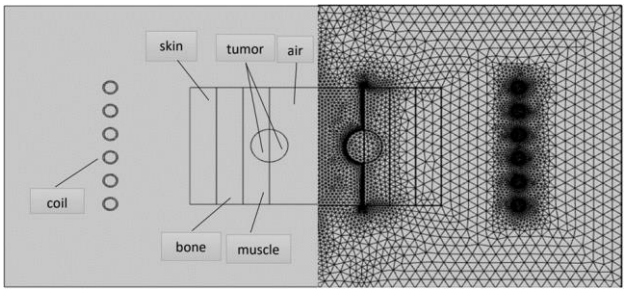

Fig. 1. View of the studied system (left) and the meshing of the problem (right).

Mathematical Model

In this study, a mathematical framework based on partial differential equations (PDEs) is utilized to model heat transfer and the interaction between magnetic nanoparticles (MNPs) and biological tissues during magnetic hyperthermia. The model simulates spatial and temporal temperature distributions across various tissue layers, including porous lung parenchyma, bone, muscle, and skin. It also accounts for the localized heat generation resulting from the presence of MNPs under an alternating magnetic field.

To evaluate the influence of physiological conditions, pulmonary ventilation (breathing) was integrated into the model to represent airflow through the porous lung structure. This consideration impacts convective heat transfer and affects both the thermal response and distribution of nanoparticles within lung tissue, thereby enhancing the model's accuracy and relevance to clinical scenarios. The finite element mesh consisted of triangular elements with refined meshing in the tumor region to capture sharp thermal gradients. A mesh independence test was performed to ensure solution accuracy, revealing minimal change in peak tumor temperature (<1%) beyond a certain mesh density. A commercial software was used to implement the model. Solver settings included a time-dependent study with backward differentiation formulas (BDF), relative tolerance of 0.001, and a maximum step size of 0.5 seconds.

The ultimate goal of the mathematical model is to optimize hyperthermia treatment parameters, such as field strength, exposure duration, and nanoparticle concentration, in order to achieve maximum therapeutic efficiency while minimizing adverse effects on surrounding healthy tissues. The heat generation within tumor tissue induced by MNPs is governed by the following equation [30–35].

$$p = \mu_0 \pi x_0 f H^2 \frac{2\pi f \tau}{1+(2\pi f \tau)^2} \quad (1)$$

In this equation, μ_0 is the permeability of free space, χ_0 is the magnetic susceptibility, H and f represent the intensity and frequency of the alternating magnetic field, and τ is the effective relaxation time, which is obtained from the following relation:

$$\tau = \frac{\tau_B \tau_N}{\tau_B + \tau_N} \quad (2)$$

In this equation, τ_B and τ_N represent the Brownian and Néel relaxation times, respectively, which are obtained from the following relations:

$$\Gamma = \frac{KV_M}{K_BT} \quad (3)$$

$$\tau_N = \frac{\sqrt{\pi}}{2}\tau_0 \frac{\exp(\Gamma)}{\sqrt{\Gamma}} \quad (4)$$

$$\tau_B = \frac{3\eta V_H}{K_BT} \quad (5)$$

In this equation, η is the viscosity of the fluid, V_h is the hydrodynamic volume of the nanoparticles, K_a is the Boltzmann constant, τ_0 is the mean relaxation time in response to thermal equilibrium, and T is the absolute temperature.

The heat transfer in biological tissues is commonly described using Pennes' bioheat equation. This equation considers the effect of blood perfusion on temperature distribution and has been widely used in thermal modeling of tumors. However, in this study, a porous media approach is adopted to better represent lung tissue characteristics, where heat exchange between blood and tissue is modeled using local thermal equilibrium assumptions.

This equation has been applied in modeling heat transfer in laryngeal tissue [29,34]:

$$\rho_1 c_1 \frac{\partial T}{\partial t} = \nabla.(k\nabla T) - \rho_b c_b w_b (T - T_b) + Q_{met} + p \text{ tumor} \quad (6)$$

$$\rho_1 c_1 \frac{\partial T}{\partial t} = \nabla.(k\nabla T) - \rho_b c_b w_b (T - T_b) + Q_{met} \text{ tissue} \quad (7)$$

Where ρ is the density, c is the specific heat, k is the tissue thermal conductivity, T is the tissue temperature, w_b is the blood perfusion, Q_{met} is the metabolic heat generation rate of the tissue, and p is the heat generated by the nanoparticles.

The introduction of a porous medium model accounts for the unique structure of lung tissue, where air-filled alveoli and capillary networks significantly influence heat transfer. This adjustment leads to a more accurate prediction of temperature gradients within the tumor and surrounding lung tissue.

The Pennes biological heat transfer equation was modified to obtain a heat transfer model based on porous media. The local thermal equilibrium assumption is also used, and the temperature field of the lung tissue can be obtained by calculation, considering that the blood and the lung tissue have the same temperature [36-40].

The equation is shown as follows:

$$(\rho c)_{eff} \frac{\partial T}{\partial t} + (\rho c)_b (u \frac{\partial T}{\partial r} + w \frac{\partial T}{\partial z}) = k_{eff} (\frac{\partial^2 T}{\partial r^2} + \frac{\partial^2 T}{\partial z^2}) + Q_{met} + Q_{ext} \quad (8)$$

$$(\rho c)_{eff} = (1 - \varphi)(\rho c)_s + \varphi(\rho c)_b \quad (9)$$

$$k_{eff} = (1 - \varphi)k_s + \varphi k_b \quad (10)$$

where ϕ is the porosity of porous media, subscripts eff, s, and b represent the effective value, solid phase (i.e., lung tissue), and liquid phase (i.e., blood) [41,42].

The boundary conditions considered for the Pennes bioheat equation are as follows:

1. At the upper and lower boundaries, the heat flux is zero ($\frac{\partial n}{\partial T} = 0$).
2. The body surface temperature is considered to be 37°C.

The porous media model is justified by the anatomical characteristics of lung parenchyma, consisting of alveolar air sacs and a dense capillary network. Thermal properties and blood perfusion rates were obtained from literature sources and represent averaged physiological values. Assumption of local thermal equilibrium (LTE) between blood and tissue was applied, which is acceptable for the scale and duration of hyperthermia treatment modeled.

Model Validation

To ensure the reliability of the simulation, a mesh independence test was conducted. Furthermore, the temperature rise trends and final thermal distributions were compared with similar simulations and experimental studies reported in the literature [14, 21, 46]. These showed good agreement, particularly in reaching therapeutic tumor temperatures (42–46 °C). This supports the credibility and applicability of the numerical framework.

We acknowledge the limitation of the 2D axisymmetric model. This choice was made to reduce computational cost while capturing the core thermal phenomena under dynamic respiratory conditions. We have now explicitly stated this in the manuscript and proposed the development of a 3D model as a future direction in the discussion section.

RESULTS

The study investigated the thermal behavior of magnetic hyperthermia in lung cancer by modeling a porous lung environment subjected to alternating magnetic fields. The respiratory cycle comprising inhalation and exhalation was included to capture realistic physiological airflow and tissue deformation.

Simulations using Fe_3O_4 nanoparticles showed effective temperature elevation within the tumor region. The porous nature of the lung tissue, combined with airflow during breathing, had a measurable impact on heat distribution. Inhalation and exhalation phases caused distinct patterns of thermal dispersion, which were analyzed separately to understand their effect on treatment efficiency.

Although tissue damage analysis was not included in this study, the temperature distributions obtained suggest that magnetic hyperthermia with Fe_3O_4 nanoparticles can achieve therapeutic temperature levels in a localized manner. These findings provide valuable insights into the optimization of nanoparticle-assisted hyperthermia for lung cancer and highlight the importance of considering respiratory mechanics in thermal treatment planning.

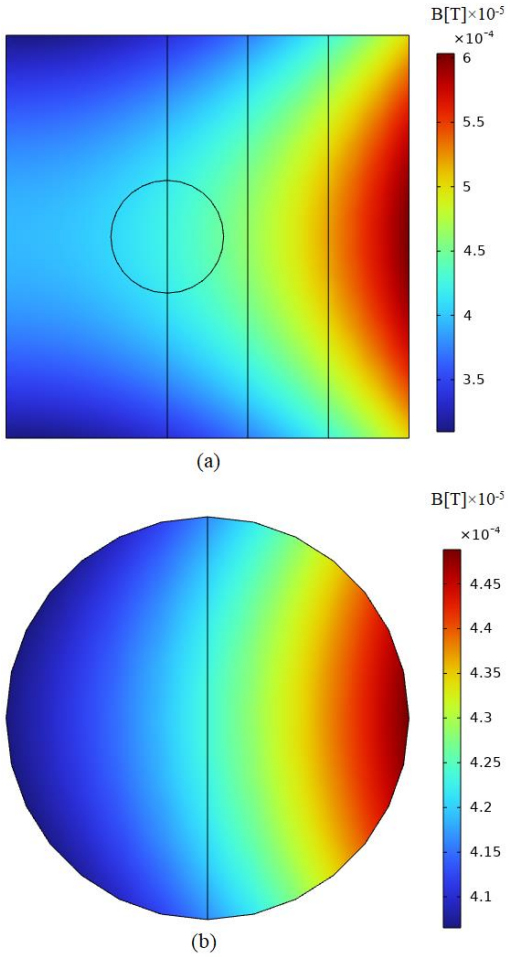

Fig. 2. Distribution of magnetic field intensity in the lung (a), and in the tumor (b).

Magnetic Field Distribution

The selection of a 300 kHz frequency is grounded in prior research demonstrating that this range optimally balances effective heat generation with minimal off target heating. Frequencies higher than this threshold risk inducing excessive thermal damage to healthy tissues, whereas lower frequencies may lead to insufficient energy absorption by the magnetic nanoparticles. Therefore, precise optimization of both frequency and magnetic field strength is essential to maximize therapeutic efficacy [47-49].

At the chosen frequency of 300 kHz, the magnetic field distribution exhibited stability and consistency for Fe_3O_4 nanoparticles across inhalation and exhalation phases. The magnetic field established a spatial gradient, with its intensity peaking centrally within the tumor and gradually diminishing towards the periphery. This near-uniform distribution facilitates controlled and consistent heat generation throughout the targeted area, thereby enhancing treatment effectiveness. Moreover, the field's stability during different respiratory phases significantly improves treatment reliability, enabling precise thermal management despite physiological motion. Prior studies have underscored the critical role of stable magnetic field distributions in optimizing nanoparticle heating performance during hyperthermia therapies.

Collectively, these results confirm that Fe_3O_4 nanoparticles benefit from a stable magnetic field at 300 kHz, ensuring efficient, localized heat deposition within the tumor while minimizing thermal exposure to adjacent healthy tissues.

Distribution of Magnetic Nanoparticle Heat in the Tumor

The simulation results illustrate the heat distribution generated by magnetic nanoparticles within the tumor, considering the lung microenvironment and respiratory airflow dynamics during inhalation and exhalation phases. The alternating magnetic field at 300 kHz frequency effectively induces localized heating, resulting in temperature elevations within the tumor tissue.

During inhalation, the increased airflow and expansion of lung tissue enhance convective heat dissipation, which slightly reduces temperature peaks, particularly at the tumor periphery. Conversely, during exhalation, reduced airflow and lung contraction facilitate more uniform heat retention within the tumor, leading to higher and more homogeneous temperature distribution. These findings demonstrate that respiratory phases significantly influence thermal profiles in lung tissue during magnetic hyperthermia. Understanding these dynamics is essential to optimize treatment parameters and ensure therapeutic temperatures (42–46 °C) are achieved consistently throughout the tumor while minimizing thermal exposure to adjacent healthy tissues.

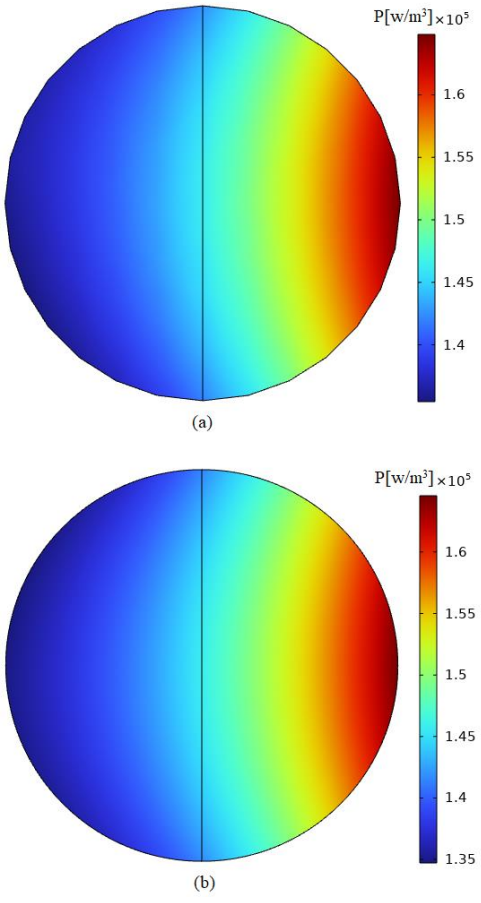

Fig. 3. Heat distribution of nanoparticles in porous lung tissue during respiratory phases: inhalation (a) and exhalation (b).

Temperature Distribution During Respiratory Phases: Inhalation and Exhalation with Cardiac Thermal Safety

The temperature distribution within the lung tumor, surrounding tissues, and adjacent cardiac region was investigated under the inhalation and exhalation phases of respiration. Considering the proximity of the heart to the thoracic cavity, maintaining cardiac thermal safety is critical during magnetic hyperthermia treatment.

Inhalation Phase: During inhalation, cooler air entering the lung enhances convective heat loss, which slightly reduces temperatures near airways and tumor margins, while the tumor core maintains therapeutic temperatures (42–46 °C) through efficient heat generation by magnetic nanoparticles. Importantly, thermal monitoring of the cardiac region indicated that the temperature remained below 39 °C, well within safe limits, thus preventing any risk of thermal injury to the heart.

Exhalation Phase: In exhalation, decreased airflow reduces convective cooling, leading to improved heat retention and a more homogeneous temperature distribution within the tumor. Despite the overall temperature increase in the lung tissue, the cardiac region's temperature stayed consistently below the critical threshold, confirming that hyperthermia treatment can be localized effectively without compromising cardiac safety.

This dual-phase analysis highlights the necessity of incorporating respiratory dynamics and adjacent organ thermal constraints into computational models. The results demonstrate that magnetic hyperthermia can be optimized to deliver sufficient tumor heating while safeguarding vital organs like the heart, supporting its potential clinical applicability in thoracic oncology.

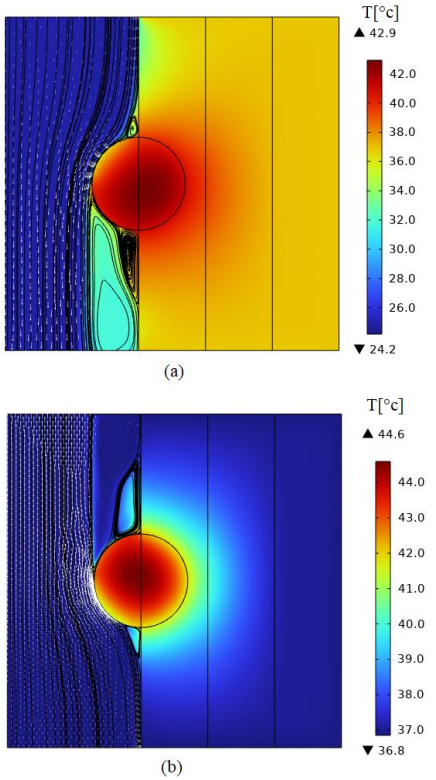

Fig. 4. Temperature distribution during respiratory phases: inhalation (a) and exhalation (b).

Temperature Contours in Lung

Figure 5 show Spatial temperature contours in a vertical lung slice during inhalation and exhalation phases. During inhalation, cooler air entering the airway results in reduced peripheral heating, particularly near the upper bronchi. In contrast, during exhalation, heat dissipation is minimized, leading to a more homogeneous thermal profile and enhanced retention within the tumor region. These dynamics illustrate the impact of respiratory airflow on thermal distribution and highlight the importance of timing in hyperthermia treatment optimization.

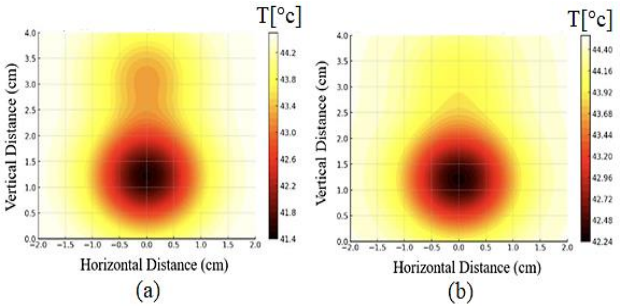

Fig. 5. Spatial temperature contours in a vertical lung slice during (a) inhalation and (b) exhalation.

Time-Dependent Temperature During Magnetic Hyperthermia

Figure 6 show Time-dependent temperature evolution in three anatomical locations during magnetic hyperthermia treatment: tumor center, tumor edge, and cardiac tissue. Fe_3O_4 nanoparticles were subjected to a 300 kHz, 300 A/m alternating magnetic field. The tumor center reached therapeutic temperatures (~44.5 °C) within 160 seconds, while the cardiac temperature remained consistently below the safety threshold of 39 °C (red dashed line), demonstrating localized heating and cardiac thermal safety.

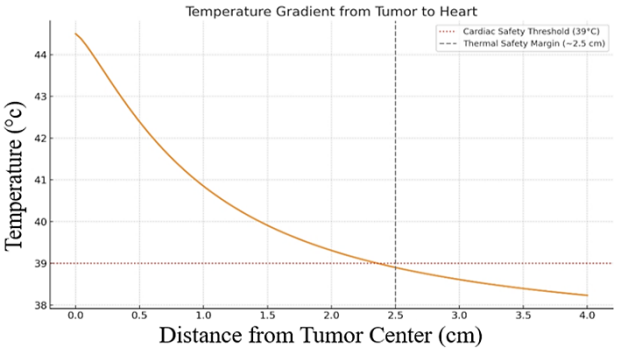

Fig. 6. Time-dependent temperature evolution in three anatomical locations during magnetic hyperthermia treatment: tumor center, tumor edge, and cardiac tissue.

DISCUSSION

Simulation results showed that airflow dynamics and lung tissue deformation significantly influence the thermal profile within the tumor region. Inhalation and exhalation phases produced distinct patterns of heat dispersion due to variations in convective flow and tissue density. These findings underscore the importance of including

respiratory mechanics in hyperthermia treatment planning, particularly for thoracic tumors located in highly dynamic anatomical regions.

Fe_3O_4 nanoparticles demonstrated the ability to generate localized heating within the therapeutic temperature range (42–46 °C), which is essential for inducing apoptosis in cancer cells. Compared to simpler models that assume static tissues and homogeneous environments, the incorporation of porous media and respiratory dynamics yielded a more accurate representation of the thermal behavior in lung tissue. These insights can guide future experimental validation and the design of optimized clinical protocols.

Although tissue damage modeling was beyond the scope of this study, the observed temperature elevations suggest a promising potential for effective tumor ablation under controlled conditions. Further investigations involving cellular response models and patient-specific geometries could strengthen the translational relevance of these findings.

Additionally, only Fe_3O_4 nanoparticles were evaluated in this study. While they are well-established in hyperthermia applications due to their magnetic properties, future work may explore alternative materials with improved biocompatibility or targeted delivery mechanisms to enhance treatment efficiency and safety.

Clinical Translation and Challenges

Magnetic nanoparticle-mediated hyperthermia holds great promise as a minimally invasive therapeutic approach for lung cancer. However, several critical challenges must be addressed to enable its safe and effective clinical translation.

Safety and Biocompatibility Concerns

The long-term biocompatibility and biodistribution of magnetic nanoparticles remain primary concerns. That Fe_3O_4 nanoparticles are widely regarded as biodegradable and relatively safe for biomedical applications. Prolonged retention in vital organs such as the liver, spleen, and lungs may induce systemic toxicity or inflammatory responses. Therefore, optimizing surface functionalization and coatings is essential to improve biocompatibility, reduce immunogenicity, and facilitate efficient nanoparticle clearance.

Targeted Delivery to Lung Tumors

Effective nanoparticle accumulation in lung tumors is challenged by physiological barriers inherent to the pulmonary system. Direct intratumoral injection can achieve high local concentrations but is invasive and less practical for widespread clinical use. Intravenous administration demands the development of active or passive targeting strategies to maximize tumor specificity and minimize off-target effects. Alternatively, inhalation-based delivery methods have emerged as a potential strategy to bypass systemic circulation and increase nanoparticle deposition directly within lung tissues, potentially improving therapeutic outcomes.

Thermal Dose Optimization and Treatment Planning

Uniform heat distribution within the tumor volume is critical for successful hyperthermia treatment. Clinical implementation is complicated by heterogeneous tumor vascularization, respiratory-induced motion, and variability in nanoparticle uptake, all of which may cause non-uniform temperature profiles and reduce treatment efficacy. Advancements in real-time thermal monitoring technologies, such as MRI-guided thermometry, are vital to dynamically adjust treatment parameters during therapy, ensuring optimized and safe thermal dosing.

Combination of Hyperthermia with Conventional Therapies

Given the complexity and heterogeneity of lung cancer, magnetic hyperthermia alone may not suffice for complete tumor eradication. However, it holds significant potential as an adjunct to established treatment modalities:

Hyperthermia and Immunotherapy: Elevated temperatures can enhance immune activation, increasing tumor antigen presentation and stimulating cytotoxic T-cell responses. This suggests a synergistic potential when combining Fe_3O_4 nanoparticle-mediated hyperthermia with immune checkpoint inhibitors (e.g., anti-PD-1/PD-L1 therapies) to improve therapeutic outcomes.

Hyperthermia and Chemotherapy: Localized hyperthermia increases chemotherapeutic drug penetration into tumor tissues, amplifying the cytotoxic effects of agents such as cisplatin and paclitaxel.

Hyperthermia and Radiotherapy: Fe_3O_4 nanoparticles serve as radiosensitizers; therefore, Fe_3O_4 nanoparticles could simultaneously potentiate hyperthermia and enhance radiotherapy efficacy by increasing DNA damage within tumor cells.

CONCLUSION

This study presented a computational investigation of magnetic hyperthermia for lung cancer treatment using Fe_3O_4 nanoparticles. By incorporating the porous structure of lung tissue and simulating respiratory dynamics, the model offered a realistic representation of heat transfer under physiological conditions. The results demonstrated that magnetic nanoparticles can effectively raise tumor temperatures to the therapeutic range (42–46 °C), while the influence of inhalation and exhalation phases plays a critical role in shaping thermal distribution.

The findings highlight the importance of considering airflow and tissue deformation in the thoracic region when designing hyperthermia-based cancer therapies. The approach provides a valuable foundation for optimizing treatment parameters such as nanoparticle concentration, magnetic field strength, and exposure duration.

Although the current study did not model tissue damage or biological response, the thermal analysis supports the potential of magnetic hyperthermia as a minimally invasive and localized treatment strategy for lung cancer. Future work may expand upon this model by integrating biological effects, patient-specific geometries, and experimental validation to move toward clinical application.

Acknowledgement

The authors appreciate the Bu-Ali Sina University for financial support through the Grant number 1002763.

Data Availability Statement

The data that support the results of this study are available from the corresponding author upon reasonable request.

References

[1] Fathalla, K., Youssef, S., Mohammed, N., 3D Deep Learning and Textural Radiomics Computational Model for Lung Cancer Staging and Tumor Phenotyping Based on Computed Tomography Volumes. Appl. Sci. 2022, 12, 6318.

[2] Sun, R., Chen, H., Wang, M., Yoshitomi, T., Takeguchi, M., Kawazoe, N., Yang, Y., Chen, G., Smart composite scaffold to synchronize magnetic hyperthermia and chemotherapy for efficient breast cancer therapy. Biomaterials. 2024; 307: 122511.

[3] Herrera, TD., Odén, J., Polo, AL., Thermoradiotherapy optimization strategies accounting for hyperthermia delivery uncertainties. Int J Radiat Oncol Biol Phys. 2024; 120(5): 1435–1447.

[4] Marczak, A., Application of nanoparticles for magnetic hyperthermia for cancer treatment the current state of knowledge. Cancers. 2024; 16: 1156.

[5] Liu, N., Pyatakov, A., Saletsky, A., Zharkov, M., Pyataev, N., Sukhorukov, G., Gun'ko, Y., Tishin, A., The 'field or frequency' dilemma in magnetic hyperthermia: The case of Zn Mn ferrite nanoparticles. J Magn Magn Mater. 2022; Aug.

[6] Włodarczyk, A., Gorgoń, S., Radoń, A., Bajdak-Rusinek, K., Magnetite nanoparticles in magnetic hyperthermia and cancer therapies: Challenges and perspectives. Nanomaterials. 2022; 12: 1807.

[7] Mao, W., Li, W., Hu, X., Tumor hyperthermia research progress and application prospect in tumoroids (Review). Mol Clin Oncol. 2024; 20: 31.

[8] Mohapatra, J., Xing, M., Liu, J., Inductive thermal effect of ferrite magnetic nanoparticles. Materials. 2019; 12: 3208.

[9] Carlton, H., Arepally, N., Healy, S., Sharma, A., Magnetic Particle Imaging-Guided Thermal Simulations for Magnetic Particle Hyperthermia. Nanomaterials, 2024; 14(12), 1059.

[10] Hendriks, L., Dingemans, A., Ruysscher, D., Aarts, M., Barberio, L., Cornelissen, R., et al., Lung Cancer in the Netherlands. Journal of Thoracic Oncology 2021, 16 (3), 355–365.

[11] Andreozzi, A., Brunese, L., Cafarchio, A., Netti, P., Vanoli, G., Effects of magnetic nanoparticle distribution in cancer therapy through hyperthermia. International Journal of Thermal Sciences. 2025; 208: 109428.

[12] Osintsev, A., Vasilchenko, I., Rodrigues, D., Characterization of ferromagnetic composite implants for tumor bed hyperthermia. IEEE Trans Magn. 2021; 57(9): 3097915.

[13] Rosensweig, R., Heating magnetic fluid with alternating magnetic field. J Magn Magn Mater. 2002; 252: 370–374.

[14] Tucci, C., Trujillo, M., Berjano, E., Iasiello, M., Andreozzi, A., Vanoli, G., Pennes' bioheat equation vs. porous media approach in computer modeling of radiofrequency tumor ablation. Sci Rep. 2021; 11(1): 5272.

[15] Alzahrani, F., Hobiny, A., Abbas, I., Marin, M., An eigenvalues approach for a two-dimensional porous medium based upon weak, normal and strong thermal conductivities. Symmetry 2020, 12, 848.

[16] Zanoli, M., Trefná, H. Suitability of eigenvalue beam-forming for discrete multi-frequency hyperthermia treatment planning. Med Phys. 2021; 48: 7410–7426.

[17] Su, T., Zhang, W., Zhang, Z., Wang, X., Zhang, S., Numerical Investigation of the Deformable Porous Media Treated by the Intermittent Microwave. Processes 2021, 9, 757.

[18] Rajan, A., Sahu, NK., Review on magnetic nanoparticle-mediated hyperthermia for cancer therapy. J Nanopart Res. 2020.

[19] Drizdal, T., vanRhoon, G., Fiser, O., Assessment of the thermal tissue models for the head and neck hyperthermia treatment planning. J Therm Biol. 2023; 115: 103625.

[20] Tang, Y., Flesch, R., Zhang, C., Numerical analysis of the effect of non-uniformity of the magnetic field produced by a solenoid on temperature distribution during magnetic hyerthermia. J Magn Magn Mater. 2018; 449: 455–460.

[21] Kandala, SK., Simulation based strategies for clinical translation of magnetic nanoparticle hyperthermia. Dissertation, The Johns Hopkins University, Baltimore, Maryland. 2017.

[22] Shoshiashvili, L., Shamatava, I., Kakulia, D., Shubitidze, F., Design and assessment of a novel biconical human-sized alternating magnetic field coil for MNP hyperthermia treatment of deep-seated cancer. Cancers. 2023; 15: 1672.

[23] Spirou, SV., CostaLima, S., Bouziotis, P., Vranješ-Djurić, S., Efthimiadou, EK., Laurenzana, A., Gobbo, OL., Recommendations for in vitro and in vivo testing of magnetic nanoparticle hyperthermia combined with radiation therapy. Nanomaterials. 2018; 8(5): 306.

[24] Napoli, N., Rodrigues, V., Davenport, P., Characterizing and modeling breathing dynamics: Flow rate, rhythm, period, and frequency. Front Physiol. 2022; 12: 772295.

[25] Shubhra, Q., Iron oxide nanoparticles in magnetic drug targeting and ferroptosis-based cancer therapy. Nanomaterials. 2023.

[26] Jiang, H., Zhou, X., Zhang, G., Temperature processing and distribution in larynx thermal inhalation injury with analogy to human airway cells: a mechanism of protection. Am J Transl Res. 2022; 14(6): 3796-3805.

[27] Elicin, O., Giger, R., Comparison of current surgical and non-surgical treatment strategies for early and

locally advanced stage glottic laryngeal cancer and their outcome. Cancers. 2020; 12: 732.
[28] Fuca, G., Reppel, L., Landoni, E., Enhancing Chimeric Antigen Receptor T-Cell Efficacy in Solid Tumors. Clin Cancer Res. 2020; 26:2444–51.
[29] Kim, Y., Park, J., Kim, J., Plain radiographic analysis of laryngeal dimensions in young children: Normal versus croup. Children. 2022; 9: 1532.
[30] Viegas, C., Pereira, D., Fonte, P., Insights into nanomedicine for head and neck cancer diagnosis and treatment. Materials. 2022; 15: 2086.
[31] Brennan, G., Bergamino, S., Pescio, M., Tofail, S., Silien, C., The effects of a varied gold shell thickness on iron oxide nanoparticle cores in magnetic manipulation, T1 and T2 MRI contrasting, and magnetic hyperthermia. Nanomaterials. 2020; 10: 2424.
[32] Attaluri, A., Jackowski, J., Sharma, A., Kandala. SK., Design and construction of a Maxwell-type induction coil for magnetic nanoparticle hyperthermia. Int J Hyperthermia. 2020; 37(1): 1–14.
[33] Ahammed, M., Yadav, K., Laxminidhi, T., Numerical study on temperature distribution during magnetic hyperthermia of different tumor tissues. Journal of Magnetism and Magnetic Materials. 2024; 593: 171868.
[34] Srinivasan, E., Liu, Y., Odion, R., Chongsathidkiet, P., Gold nanostars obviate limitations to laser interstitial thermal therapy (LITT) for the treatment of intracranial tumors. Clinical Cancer Research. 2023; 29(16): 3214–3224.
[35] Tucci, C., Trujillo, M., Berjano, E., Iasiello, M., Andreozzi, A., Vanoli, G., Pennes' bioheat equation vs. porous media approach in computer modeling of radiofrequency tumor ablation. Sci. Rep. 2021, 11, 5272.
[36] Etminan, A., Dahaghin, A., Emadiyanrazavi, S., Salimibani, M., Simulation of heat transfer, mass transfer, and tissue damage in magnetic nanoparticle hyperthermia with blood vessels. Journal of Thermal Biology. 2022; 110: 103371.
[37] Mai, X., Wu, N., Nan, Q., Bi, S., Simulation study of microwave ablation of porous lung tissue. Appl. Sci. 2023; 13: 625.
[38] Gazel, D., Akdoğan, H., Manay, A., The potential of therapeutic hyperthermia to eradicate Staphylococcus aureus bacteria; an in vitro study. Journal of Thermal Biology. 2024; 120: 103812.
[39] Drizdal, T., Rhoon, G., Fiser, O., Vrba, D., Assessment of the thermal tissue models for the head and neck hyperthermia treatment planning. Journal of Thermal Biology. 2023; 115: 103625.
[40] Guan, L., Torres-Saavedra, P., Zhao, X., Major, M., Holmes, B., Association between locoregional failure and NFE2L2/KEAP1/CUL3 mutations in NRG/RTOG 9512: A randomized trial of radiation fractionation in T2N0 glottic cancer. *Clinical Cancer Research*. 2025, CCR-24-2334.
[41] Abdulrasool, A., Abbas, A., Abdullah, W., The cooling effect of blood flow during hyperthermia treatment. Journal of Thermal Biology. 2023; 114: 103581.
[42] Subeg, S., Neeraj, K., Effect of arterial flow on heat transfer during magnetic hyperthermia application. Fluid Mechanics and Fluid Power. 2024; 4: 755–766.
[43] Mehul, C., Xianghong, M., Jia, Y., Optimizing magnetic fields and coil designs for magnetic hyperthermia breast cancer treatment. Advances in Digital Health and Medical Bioengineering. 2024; 3: 3–12.
[44] Izaz, R., Heung, S., Piotr, G., Advances in finite element analysis for cancer therapy focusing on magnetic nanoparticle hyperthermia. Multiscale Science and Engineering. 2024; 6: 113–123.
[45] Jaswantsing, R., Anil, N., Sanjay, N., Feasibility study for local hyperthermia of breast tumors: A 2D modeling approach. Intelligent Computing and Networking. 2022; 260–271.
[46] Suleman, M., Riaz, S., Jalil, R., A mathematical modeling approach toward magnetic fluid hyperthermia of cancer and unfolding heating mechanism. Journal of Thermal Analysis and Calorimetry. 2021; 146: 1193–1219.
[47] Soheil, S., Dehkordi, M., Ahmadikia, H., Improved liver cancer hyperthermia treatment and optimized microwave antenna power with magnetic nanoparticles. Heat and Mass Transfer. 2024; 60: 1235–1250.
[48] Kubo, Y., Nozaki, R., Igaue, S., Utsunomiya, D., Neoadjuvant chemotherapy improves feasibility of larynx preservation and prognosis in resectable locally advanced cervical esophageal cancer. Annals of Surgical Oncology. 2024; 31: 5083–5091.
[49] Fucà, G., Reppel, L., Landoni, E., Savoldo, B., Dotti, G., Enhancing chimeric antigen receptor T-cell efficacy in solid tumors. Clinical Cancer Research. 2020; 26(11): 2444–2451.
[50] Ou, J., Zhu, X., Chen, P., Du, Peng X., A Randomised Phase II Trial of Vitamin C Synergy with Hyperthermia in Patients with Advanced Non-Small-Cell Lung Cancer. Journal of Thoracic Oncology 2019, 14 (10), S926–S927.
[51] Hendriks, L., Dingemans, C., Ruysscher, M., Aarts, M., Barberio, L., Cornelissen, R., Lung Cancer in the Netherlands. Journal of Thoracic Oncology 2021; 16 (3), 355–365.